VNU Journal of Science: Mathematics - Physics

Journal homepage: https://js.vnu.edu.vn/MaP

Original Article

Study of the Photoluminescence Enhancement/Quenching of ZnS:Mn^{2+} in the Presence of Au/Ag Nanoparticles Synthesized by Pulse Laser Ablation in Solution

Tran Trong Duc, Bui Hong Van, Nguyen The Binh*

University of Science, Vietnam National University, Hanoi,
334 Nguyen Trai, Thanh Xuan, Hanoi, Vietnam

Received 14 March 2022
Revised 28 March 2022; Accepted 31 March 2022

Abstract: Gold (Au) and silver (Ag) nanoparticles were synthesized by laser ablation in water. The average sizes of Au and Ag nanoparticles are of 18.4 nm and 21.8 nm, respectively. ZnS:Mn^{2+} nanoparticles with average size of 3-5 nm were prepared by co-precipitation method. The photoluminescence of ZnS:Mn^{2+}solution in mixture with Au (Ag) nanoparticle colloids was investigated. The quenching effect on Mn^{2+} emission at 601 nm band was observed in the presence of the Au and Ag nanoparticles, while the D-A emission at 445 nm band was enhanced and blue shifted by Au nanoparticles.

Keywords: Laser ablation, metal enhanced fluorescence, plasmonic nanostructure.

1. Introduction

Metal Enhanced Fluorescence (MEF) was first discovered in the 1970 s [1-3] and has been increasingly developed because of its widely applications in fluorescence, bio-chemical, molecule biology, environments etc. [3-11]. MEF was also referred to as surface-enhanced fluorescence, plasmon-enhanced fluorescence, and radiative decay engineering that arises from a dipole interaction between a fluorophore and a local surface plasmon (LSP), while incoming radiation interacts with both the metal surface and the fluorophore. Besides the enhancement, the fluorescence quenching is of strong interest

* Corresponding author.
E-mail address: thebinh@hus.edu.vn

https//doi.org/10.25073/2588-1124/vnumap.4708

for applications in scanning probe microscopy, surface enhanced Raman spectroscopy and biosensing etc. [4, 5].

The actual MEF mechanism today is being discussed and debated. There are two main mechanisms of MEF: (i) The enhancement of the incident excitation field; and (ii) The enhancement of the emission rate. In the first mechanism, metal nanoparticles can greatly enhance the local excitation intensities by LSP and as a consequence, the luminescence efficiency is enhanced. In the second mechanism, the presence of metallic particles rerults in effects on the radiative decay rate of a nearby fluorophore. The photoluminescence of a fluorophore can be enhanced or quenched depending on the size and shape of the metal NPs, the orientation of the fluorophore's molecular dipole moment, and the overlap of the fluorophore emission spectrum with the spectrum of metal NPs' surface plasmon resonance [7-9]. The metal nanoparticles themselves can radiate the coupled quanta by the coupling of fluorophore and metal in both the ground and excited state [10,12] or by the scattering mode of the nanoparticle due to the inefficient overlap of the fluorophore emission spectrum and the scattering portion of the nanoparticle extinction [7,11].

Unlike surface enhanced Raman scattering (SERS), MEF requires an optimal distance between fluorophore's molecules and the metal's surface depending on the fluorophore and plasmonic nanostructure (around 10-20 nm) [13-15]. At too short distances, the fluorescence of the fluorophore is quenched, and at too far distances, the dipole coupling between the fluorophore and the LPS is too weak for a fluorescence enhancement. For this reason, core–shell nanoparticles have been recently employed in MEF. In the core–shell nanoparticle structures for MEF, the core is composed of a plasmonic metal and the shell is a dielectric material such as silicon dioxide where the dielectric shell provides a optimal spacer for the MEF effect.

In this work, we investigated the photoluminescence of ZnS:Mn^{2+} nanoparticles by mixing ZnS:Mn^{2+} solution with metal nanoparticle colloids in water with different concetrations of metal (Au, Ag) nanoparticles (NPs). The Au NPs and Ag NPs were synthesized by pulsed laser ablation (PLA) in water. By varying the concetrations of Au (Ag) nanoparticles in the ZnS:Mn^{2+} solution one can find-out an optimum concentration for the MEF effect.

ZnS:Mn^{2+} is one of the most important materials for luminescence due to its wide application in electroluminescence and cathodoluminescence displays. The MEF investigation of ZnS:Mn^{2+} may be useful for wider applications of this luminescence material.

2. Experimental

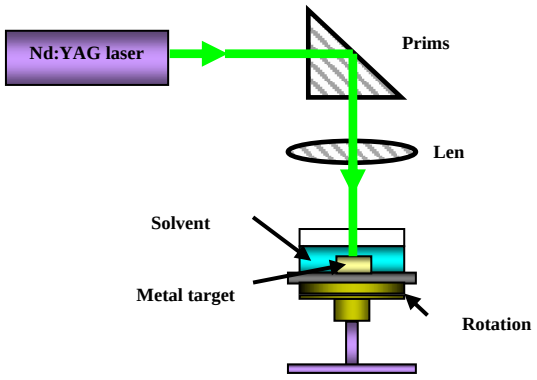

Figure 1. PLA system used for synthesizing noble metal NPs.

Gold and silver NPs were prepared by laser ablation of Au and Ag metal plates put in water. The noble metal plate (99.9% in purity) was placed in a glass cuvette filled with 10 ml water. The fundamental wavelength (1064 nm) of the Quanta Ray Pro 230 Nd:YAG pulsed laser, with pulse duration of 8 ns, repetition rate of 10 Hz was focused on the metal plate by a lens having the focal length of 100 mm. The experimental scheme is shown in Figure 1.

The photoluminescence of Zn:Mn^{2+} was collected by Princeton's SpectraSense Spectrometer. The experimental scheme is shown in Figure 2.

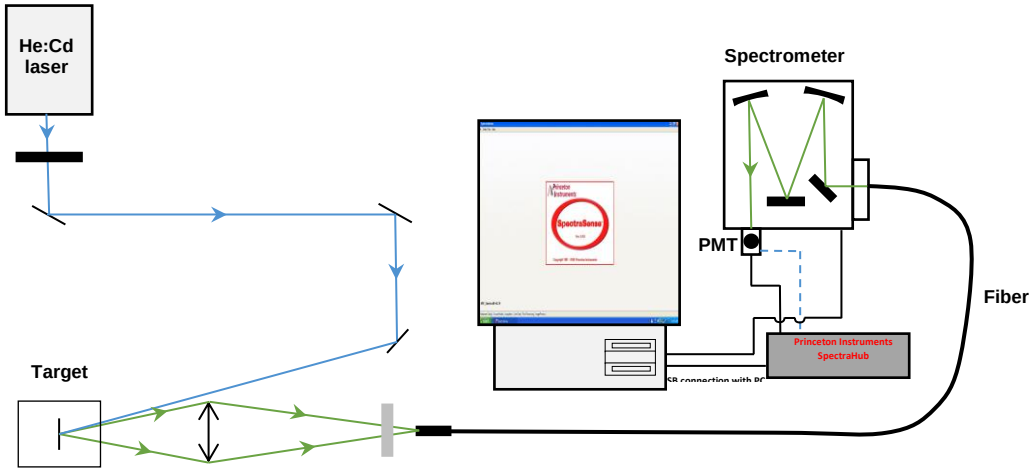

Figure 2. Experimental setup for photoluminescence spectrum collection.

The absorption spectra of nanoparticle colloids were recorded by a Shimadzu UV-2450 spectrometer. The chemical composition of NPs was investigated by energy-dispersive X-ray spectroscopy (EDX). The morphology of the NPs was studied by transmission electron microscopy (TEM) in a JEM 1010-JEOL. The size of NPs was determined by ImagieJ 1.50i software of Wayne Rasband (National Institutes of Health, USA). The size distribution was calculated and obtained by OriginPro 2019b softwares.

The nanoparticles Mn-doped ZnS with Mn content of 8 mol% were synthesized by a co-precipitation method. $Zn(CH_3COO)_2.2H_2O$,$Mn(CH_3COO)_2.4H_2O$ and Na_2S were dissolved in distilled water to create $Zn(CH_3COO)$20.1M (A), $Mn(CH_3COO)$20.1M (B) and Na_2S(C) solutions. An additional amount of CH3COOH was droped into the solution to produce a pH = 3.5 solution (D). After that, the solution D was slowly dropped into the solution C. The mixtures were stirred continuously for 30 minutes at each steps above. These precipitations were washed by distilled water, separated by centrifuging with a speed of 2500 rpm, dried at 80˚ for 10h and then annealed at 120 ºC for 10 h in the air. The crystalline structure analysis was carried-out on a X-ray diffractometer "XD8 Advance Buker system" using Cu-Kα (λ= 1.5046˚ A) [16]. The nanoparticles of Mn:ZnS^{2+} 8 mol% with the average size of 3-5 nm showed two distinctive fluorescence bands at 445 nm and 601 nm, corresponding to the emission from donor-acceptor D-A pairs and the emission from the $^4T_1(^4G)$– $^6A_1$ (^6S) transition of Mn^{2+}[16-18].

To study MEF effect of Ag (Au) NPs on ZnS:Mn^{2+}: 0.100 g of ZnS:Mn^{2+} 8 mol% was dissolved in 100 ml water, then the solution was continuously put under ultra-sonic wave for 60 minutes and ZX3 Advanced Vortex Mixer for 30 minutes. The mixtures of Ag (Au) NP colloids in water and ZnS:Mn^{2+} 8 mol% solutions were prepared with an Ag(Au)NP/ ZnS:Mn volume ratio range of 0.05% to 0.20%. These solutions were mixed by Ultra-sonic wave and ZX3 Advanced Vortex Mixer for another 10 minutes before PL excitation.

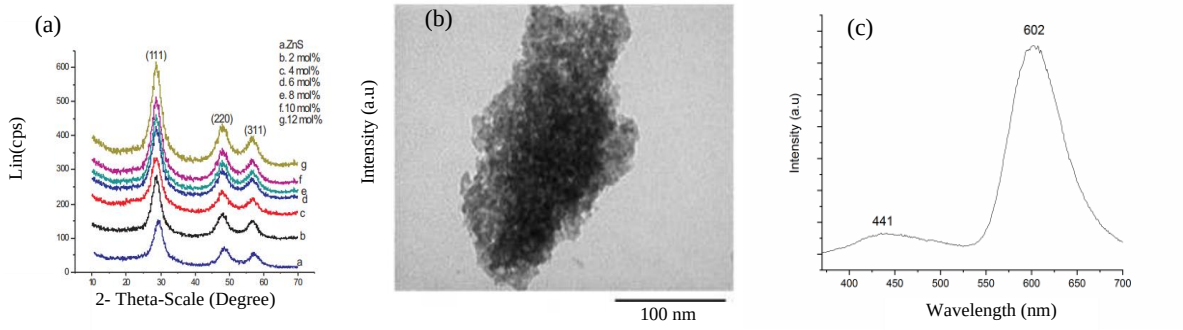

Figure 3. (a) The XRD patterns of ZnS, ZnS:Mn nanoparticles with different Mn contents; (b) TEM image of ZnS:Mn nanoparticles (C_{mn} = 8 mol%)[19]; (c) PL spectra of ZnS:Mn nanoparticles.

3. Results and Discussion

3.1. Preparation of Ag, Au Nanoparticles

3.1.1. Preparation of Ag Nanoparticles

Using a Nd:YAG laser with the fundamental wavelength 1064 nm, average power of 450 mW and irradiation time of 15 minutes, Ag NPs in water were prepared.

The absorption spectra, TEM image and size distribution of Ag NPs in water are presented in Figure 4. The concentration of Ag NPs colloid measured by Atomic absorption spectroscopy (AAS) is 32.04 mg/l. The Ag NPs have surface plasmon absorption peak at about 401 nm and mean diameter of 18.4 nm with size ranging from 3.5 to 65.6 nm.

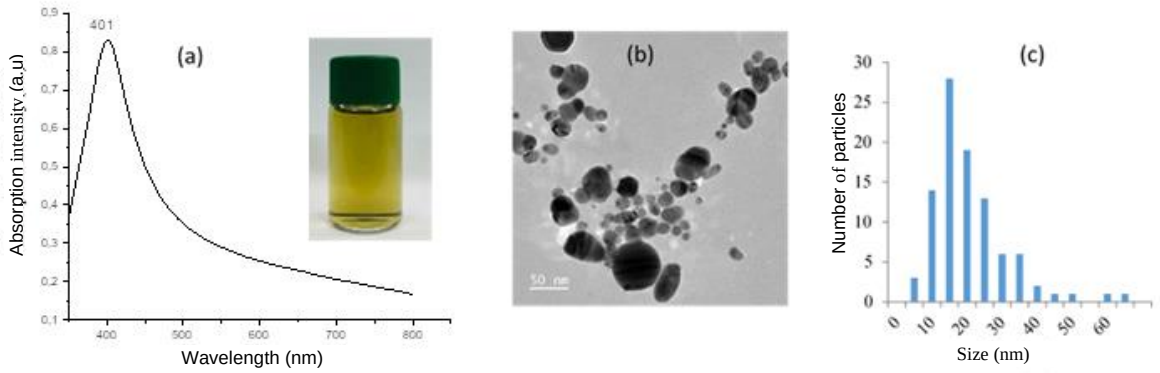

Figure 4. (a) Absorption spectra, (b) TEM image, and (c) size distribution of Ag NPs in water.

3.1.2. Preparation of Au Nanoparticles

Using average power of 450 mW and irradiation time of 15 minutes, Au NPs in water were also prepared. TEM image in Figure 5 shows that Au NPs have a near spherical shape with a mean diameter of 21.8 nm and size ranging from 5.4 to 58.7 nm.

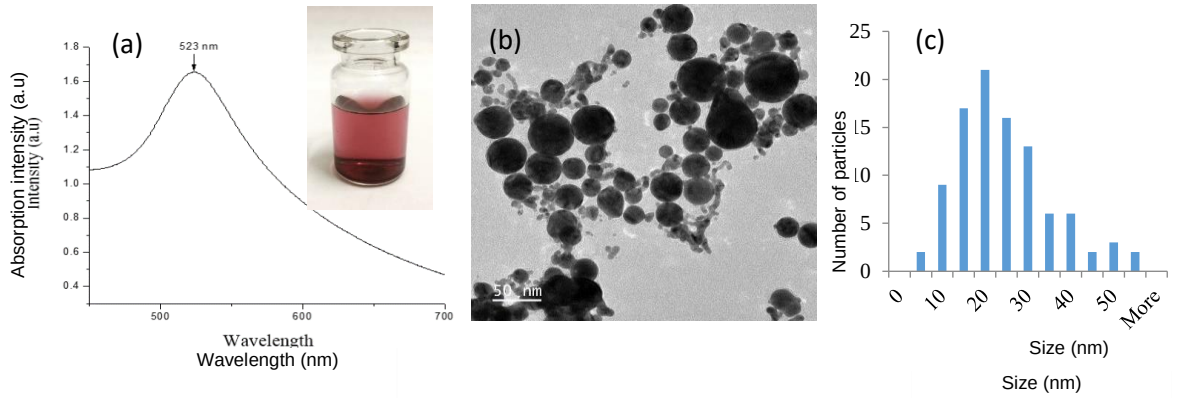

Figure 5. (a) The absorption spectra, (b) TEM image and (c) size distribution of Au NPs in water.

The absorption spectrum of Au NPs exhibits a characteristic peak of the surface plasmon absorption band at about 523 nm. From AAS measurement, the concentration of the Au NPs colloid was found to be of 97.4 mg/l.

3.2. Photoluminescence of ZnS:Mn^{2+} in the Presence of Ag NPs and Au NPs

3.2.1. PL of ZnS:Mn^{2+} in the Presence of Ag NPs

By using the 325 nm wavelength of He:Cd laser as the excited light source , we have studied the PL spectra of ZnS: Mn^{2+} solutions with different concentrations of Ag NPs. As shown in Figure 6, the intensity of both D-A emission at 445 nm band and Mn^{2+} emission at 601 nm band were decreased when the Ag NP/ ZnS:Mn volume ratios increased from 0.05% to 0.25%.

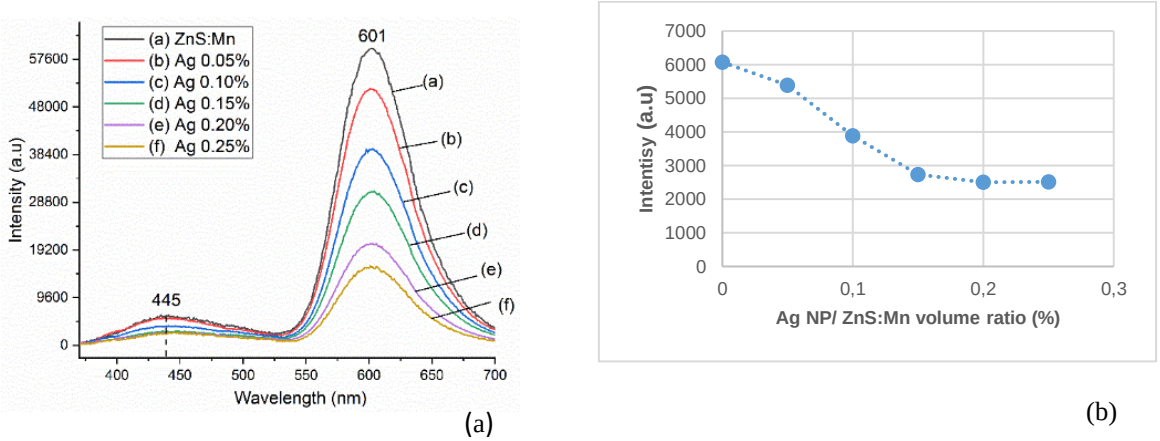

Figure 6. (a) PL spectra of ZnS: Mn^{2+} solutions with different Ag NP/ ZnS:Mn volume ratios from 0.05% to 0.25%. (b) The intensity of 445 nm PL band with the increasing Ag Np concentrations.

The decrease in the PL intensity of 445 nm band (Figure 6b) can be explained due to the non-radiative absorption of Ag NPs. The D-A emission band at 445 nm is partially overlapped with the Ag surface plasmon absorption band at 401 nm, which causes the quenching effect on the D-A emission.

To explain the quenching effect on Mn^{2+} emission at 601 nm band, we consider the mechanism of Mn^{2+} emission.

Figure 7 illustrates a diagram of energy levels, the mechanism of excitation energy transferring and the radiative transition at 601 nm band of Mn^{2+} in Mn- doped ZnS crystal. The excitation by the radiation of 325 nm with photon energy larger than band gap energy of ZnS crystal causes an indirect excitation of electrons in $3d^5$ unfulfilled shell of Mn^{2+} ions $^4T_2(^4D)$, $^4A_1(^4G)$ -$^4E_1(^4G)$, $^4T_2(^4G)$. After that, by a non-radiative transition, the electrons transit into $^4T_1(^4G)$ state and finally transit into ground state $^6A_1$ (^6S) to emit the yellow-orange band at 601 nm [16, 18]. In the PLE spectra monitoring at 601 nm of Mn-doped ZnS, the absorption band near the band edge shifts towards to the longer wavelengths at 432, 466, 497 nm (Figure 7).

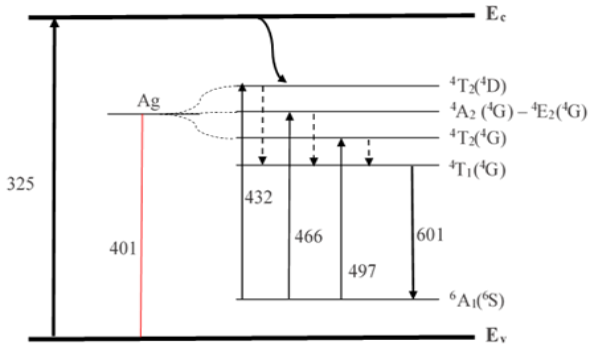

Figure 7. Diagram of energy levels, the mechanism of excitation energy transferring and the radiative transition at 601 nm band of Mn^{2+} in Mn- doped ZnS crystal.

Those are assigned to absorption transitions of electrons from $^6A_1$ (^6S) ground state to excited states $^4T_2(^4D)$, $^4A_1(^4G)$ -$^4E_1(^4G)$, $^4T_2(^4G)$ [18]. Due to the presence of Ag NPs with the surface plasmon absorption band of 401 nm, there was a Fröster energy transfer [19-20] from those excited states to Ag NPs in non-radiative transition processes that eventually decrease the cumulative population in $^4T_1(^4G)$ state and lead to the decrease in intensity of 601 nm band.

3.2.2. PL of ZnS:Mn^{2+} in the Presence of Au NPs

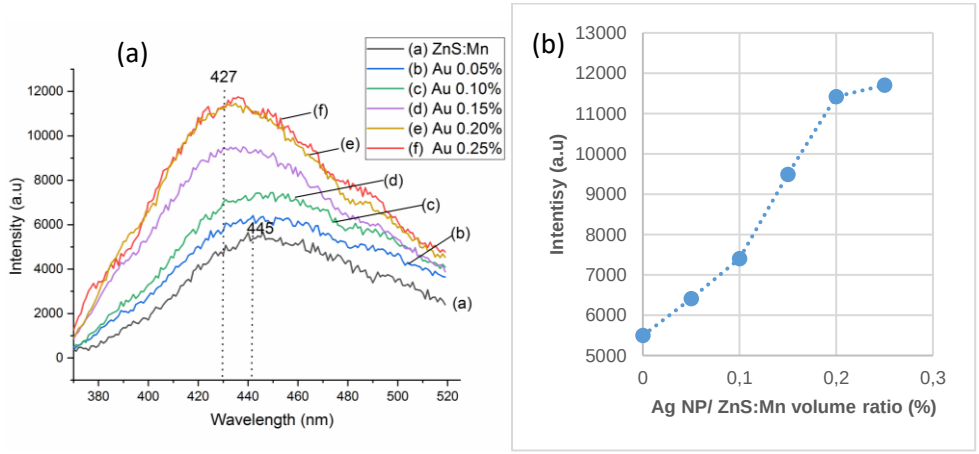

Figure 8. (a) PL spectra of the ZnS:Mn at D-A emission band with different Au NP/ZnS:Mn volume ratios (b) The intensity of 445 nm PL band with the increasing Au Np concentrations.

Using the same PL spectrophotometer, we have studied the PL spectra of ZnS:Mn^{2+} solutions with different concentrations of Au NPs. The results showed that when the Au NP/ ZnS:Mn volume ratio increased from 0.05% to 0.25 %, the photoluminescence intensity was decreased at 601 band meanwhile the intensity of D-A emission at 445 nm was enhanced and appears to be saturated as the Au NP/ ZnS:Mn volume ratios increases more than 0.20 % (Figure 8b). Furthermore, the D-A emission peak was slightly shifted from 445 nm to 427 nm with the increasing Au NP/ ZnS:Mn volume ratios (Figure 8a).

The photoluminescence enhancement or quenching depends on the coupling of the light emission with the surface plasmon resonance of Au nanoparticles. The light emission may be enhanced when surface plasmon resonance scattering dominates over the absorption process and it will be quenched due to a nonradiative dissipation of surface plasmon absorption [20]. According to an investigation of Messinger et al., [21], the scattering intensity corresponding to surface plasmon absorption peak of a given size Au nanoparticles is largely reduced, while the scattering is greatly increased at the shorter wavelength range. For the Au nanoparticles with average size of around 20 nm the scattering is very weak at wavelengths longer than 520 nm and stronger at wavelengths shorter than 520 nm. In the PL spectrum of ZnS:Mn^{2+}, the Mn^{2+} emission peak at 601 nm is partially overlapped with the surface plasmon absorption of Au NPs (520 nm) but far from the scattering wavelength range of Au nanoparticles. This is the reason why the Mn^{2+} emission at 601 nm was quenched. Meanwhile, the D-A emission peak at 445 nm is hardly overlapped with the surface plasmon absorption but largely overlapped with the scattering of Au nanoparticles. This is the reason why the D-A emission at 445 nm was enhanced in the presence of Au nanoparticles [20, 21]. This observation is also in accordance with the results reported in [15] for photoluminescence of Au/silica/ZnS:Mn core-shell and in [18] for photoluminescence of Au–ZnS nanocomposite.

The blue D-A emission at 445 nm is an important component for white light and color display applications of ZnS:Mn^{2+} material, therefor the enhancement of the blue D-A emission by Au NPs may be useful for a wider application of this luminescence material in display.

4. Conclusion

The photoluminescence enhancement and quenching of ZnS:Mn^{2+} solutions in mixture with Au NPs and Ag NPs synthesized by pulsed laser ablation in water were investigated. The quenching effect on Mn^{2+} emission at 601 nm was observed in the mixtures of ZnS:Mn^{2+}solutions and colloidal Ag (Au) NPs. However, the D-A emission of ZnS:Mn^{2+}solution at 445 nm was enhanced and blue shifted by embedding Au nanoparticles, whereas it was quenched by embedding Ag nanoparticles. The MEF effect was observed dependent on the Ag (Au) NPs concentration in the ZnS:Mn^{2+} solutions. The obtained results suggest a simple way to get MEF effect of ZnS:Mn^{2+} by using Ag NPs and Au NPs synthesized by PLA .

Acknowledgements

This research is funded by the University of Science, Vietnam National University, Hanoi under project number TN.21.06

Reference

[1] M. R. Philpott, Effect of Surface Plasmons on Transitions in Molecules, J. Chem. Phys., Vol. 62, No. 5, 1975, pp. 1812-1817, https://doi.org/10.1063/1.430708.

[2] H. Kuhn, Classical Aspects of Energy Transfer in Molecular Systems, J. Chem. Phys., Vol. 53, No. 1, 1970, pp. 101-108, https://doi.org/10.1063/1.1673749.

[3] C. Geddes, J. Lakowicz, Editorial: Metal-Enhanced Fluorescence, J. Fluorescence, Vol. 12, No. 2, 2002, pp. 121-129, https://doi.org/10.1023/A:1016875709579.

[4] J. R. Lakowicz, Radiative Decay Engineering: Biophysical and Biomedical Applications, Anal. Biochem. 298(1), 2001, pp. 1-24, https://doi.org/10.1006/abio.2001.5377.

[5] J. R. Lakowicz, B. Shen, Z. Gryczynski, S. D'Auria, I. Gryczynski, Intrinsic Fluorescence from DNA Can Be Enhanced by Metallic Particles, Biochem. Biophys. Res. Commun., Vol. 286, No. 5, 2001, pp. 875-879, https://doi.org/10.1006/bbrc.2001.5445.

[6] K. Aslan, C. D. Geddes, Metal-Enhanced Fluorescence: Progress Towards A Unified Plasmon-Fluorophore Description, John Wiley & Sons, Inc., Hoboken, New Jersey, 2010, pp. 1-23.

[7] E. C. L. Ru et al., Spectral Profile Modifications in Metal-Enhanced Fluorescence, John Wiley & Sons, Inc., Hoboken, New Jersey, 2010, pp. 25-65.

[8] C. D. Geddes, John Wiley and Sons, New Jersey, Metal-Enhanced Fluorescence, 2010, pp. 625.

[9] A. I. Dragan, B. Mali, C. D. Geddes, Wavelength-Dependent Metal-Enhanced Fluorescence Using Synchronous Spectral Analysis, Chem. Phys. Lett., 2013, pp. 168-172, https://doi.org/10.1016/J.Cplett.2012.11.035.

[10] M. R.Vasic, E. Spruijt, Z. Popovic, K. Overgaag, B. V. Lagen, B. Grandidier, D. Vanmaekelbergh, D. D. Gutierrez, L. D. Cola, and H. Zuilhof, Amine-Terminated Silicon Nanoparticles: Synthesis, Optical Properties and Their Use in Bioimaging, J. Mater. Chem. 19(33), 2009, pp. 5926-5933, https://doi.org/10.1039/B902671a.

[11] J. Knipping, H. Wiggers, B. Rellinghaus, P. Roth, D. Konjhodzic, and C. Meier, Synthesis of High Purity Silicon Nanoparticles in A Low Pressure Microwave Reactor, J. Nanosci. Nanotechnol., Vol. 4, No. 8, 2004, pp. 1039-1044, https://doi.org/ 10.1166/jnn.2004.149.

[12] X. Zhang, D. Neiner, S. Wang, A. V. Louie, S. M. Kauzlarich, A New Solution Route to Hydrogen-Terminated Silicon Nanoparticles: Synthesis, Functionalization and Water Stability, Nanotechnology, Vol. 18, No. 9, 2007, pp. 095601, https://doi.org/10.1088/0957-4484/18/9/095601.

[13] W. Deng, F. Xie, H. T. M. C. M. Baltarac, E. M. Goldys, Metal-Enhanced Fluorescence in The Life Sciences: Here, Now and Beyond, Physical Chemistry Chemical Physics, Vol. 15, 2013, pp. 15695-15708, https://doi.org/10.1039/C3cp50206f.

[14] P. Strobbia; E. R. Languirand; B. M. Cullum, Recent Advances in Plasmonic Nanostructure for Sensing: A Review, Opt. Eng., Vol. 54, No. 10, 2015, pp. 100902, https://doi.org/ 10.1117/1.Oe.54.10.100902.

[15] L. Ma, W. Chen, Luminescence Enhancement and Quenching in ZnS:Mn by Au Nanoparticles, Journal of Applied Physics, Vol. 107, 2010, pp. 123513, https://doi.org/10.1063/1.3432740.

[16] B. H. Van, P. V. Ben, H. N. Nhat, N. T. Uyen, T. T. Thi, The Optical Property of Mn-Doped ZnS Nanoparticles Synthesized by A Co-Precipitation Method, Communications In Physics, Vol. 22, No. 2, 2012, pp. 167-173, https://doi.org/10.15625/0868-3166/22/2/1617.

[17] W. Chen, R. Sammynaiken, Y. N. Huang, J. O. Malm, R. Wallenberg, J. O. Bovin, V. Zwiller, N. A. Kotov, Crystal Field, Phonon Coupling and Emission Shift of Mn2+ in Zns:Mn Nanoparticles, J. Appl. Phys., Vol. 89, 2001, pp. 1120, https://doi.org/10.1063/1.1332795.

[18] C. Yang, Y. Zhou, G. An, X. Zhao, Surface Plasmon Induced Photoluminescence Enhancement in The Au–ZnS Nanocomposite, Optical Materialsl, Vol. 5, No. 12, 2013, pp. 2551-2555, https://doi.org/10.1016/j.optmat.2013.07.023.

[19] T. Ozel, S. Nizamoglu, M. A. Sefunc, O. Samarskaya, I. O. Ozel, E. Mutlugun, V. Lesnyak, N. Gaponik, A. Eychmüller, S. V. Gaponenko, H. V. Demir, Anisotropic Emission from Multilayered Plasmon Resonator Nanocomposites of Isotropic Semiconductor Quantum Dots, Acs Nano, Vol. 5, No. 2, 2011, pp. 1328-1334, https://doi.org/10.1021/Nn1030324.

[20] P. Viste, J. Plain, R. Jaffiol, A. Vial, P. M. Adam, P. Royer, Enhancement and Quenching Regimes in Metal-Semiconductor Hybrid Optical Nanosources, Acs Nano Vol. 4, 2010, pp. 759-764, https://doi.org/10.1021/Nn901294d.

[21] B. J. Messinger, K. U. V. Raben, R. K. Chang, P. W. Barber, Local Fields at The Surface of Noble-Metal Microspheres, Phys. Rev. B 24, Vol. 24, No. 2,1981, pp. 649-657, https://doi.org/10.1103/Physrevb.24.649.